

# Trait-based approaches reveal fungal adaptations to nutrient-limiting conditions

Tessa Camenzind <sup>1,2\*</sup> Anika Lehmann,<sup>1,2</sup>  
Janet Ahland,<sup>1</sup> Stephanie Rumpel<sup>1</sup> and  
Matthias C. Rillig<sup>1,2</sup>

<sup>1</sup>Institute of Biology, Freie Universität Berlin, Berlin, Altensteinstr. 6, 14195, Germany.

<sup>2</sup>Berlin-Brandenburg Institute of Advanced Biodiversity Research (BBIB), Berlin, 14195, Germany.

## Summary

The dependency of microbial activity on nutrient availability in soil is only partly understood, but highly relevant for nutrient cycling dynamics. In order to achieve more insight on microbial adaptations to nutrient limiting conditions, precise physiological knowledge is needed. Therefore, we developed an experimental system assessing traits of 16 saprobic fungal isolates in nitrogen (N) limited conditions. We tested the hypotheses that (1) fungal traits are negatively affected by N deficiency to a similar extent and (2) fungal isolates respond in a phylogenetically conserved fashion. Indeed, mycelial density, spore production and fungal activity (respiration and enzymatic activity) responded similarly to limiting conditions by an overall linear decrease. By contrast, mycelial extension and hyphal elongation peaked at lowest N supply (C:N 200), causing maximal biomass production at intermediate N contents. Optimal N supply rates differed among isolates, but only the extent of growth reduction was phylogenetically conserved. In conclusion, growth responses appeared as a switch from explorative growth in low nutrient conditions to exploitative growth in nutrient-rich patches, as also supported by responses to phosphorus and carbon limitations. This detailed trait-based pattern will not only improve fungal growth models, but also may facilitate interpretations of microbial responses observed in field studies.

## Introduction

The fungal lifestyle of exploration and invasion by mycelial growth is unique and extraordinarily successful

(Moore *et al.*, 2011; Fricker *et al.*, 2017). In the heterogeneous environment of soil, fungal hyphae of one individual encounter a heterogeneous soil matrix, connecting patches of different composition and substrate quality (Boddy, 1999). Fungi can translocate elements within their mycelium, and adjust colonization intensity to the quality of the substrate, likely allowing them to cope with patchily distributed nutrient availability, including locally limited elements (Ritz, 1995; Falconer *et al.*, 2007). Nevertheless, fungi require elements in physiologically defined stoichiometric ratios (Elser *et al.*, 1996). To access elements in soil, fungi depend on a range of enzymes, making them key players in soil nutrient cycles and soil carbon (C) sequestration (Cooke and Whipps, 1993). Together with soil bacteria, fungal activity and element demands determine the prevalence of mineralization versus immobilization rates in soil, regulating nutrient availability of plants, and thus primary productivity (Manzoni *et al.*, 2010).

Nitrogen (N) and/or phosphorus (P) availability limits plant growth in most natural systems (Vitousek and Howarth, 1991; Augusto *et al.*, 2017). Compared with the detailed experimental evidence for plant nutrient demands, there is still no consistent theoretical framework for microbial nutrient limitations or responses to shifting nutrient levels in soil (Rousk and Bengtson, 2014). This is problematic in the context of environmental change because microbial responses also determine ecosystem outcomes (Hu *et al.*, 2001; Coskun *et al.*, 2016). While limitations especially by N for microbial activity and biomass build-up are generally assumed in theoretical models (Hartman and Richardson, 2013), N fertilization experiments show predominantly negative effects of N enrichment, which only partially stem from negative side effects, such as acidification and osmotic stress (Treseder, 2008; Riggs and Hobbie, 2016; Averill and Waring, 2018). In addition, microbial respiration often negatively correlates with soil N contents, resulting in lower microbial carbon-use-efficiency (CUE) in N-limited substrates (Manzoni *et al.*, 2012; Spohn and Chodak, 2015). In parallel to high respiration rates in N deficient soils, microbial enzymatic activity also may increase: Assuming N is a limiting factor in soil, those counterintuitive effects are interpreted as ‘waste respiration’ and ‘N mining’ in low

Received 31 October, 2019; revised 6 May, 2020; accepted 15 June, 2020. \*For correspondence. E-mail [tessac@zedat.fu-berlin.de](mailto:tessac@zedat.fu-berlin.de)

N conditions by some authors (Schimel and Weintraub, 2003; Craine *et al.*, 2007).

Specifically for soil saprobic fungi, results are similarly inconsistent. In natural environments, many substrates exhibit much wider C:N ratios than fungi, for example, wood or also some litter types. Thus, fungi are supposed to compete with other organism groups for mineralized N (Watkinson *et al.*, 1981; McGroddy *et al.*, 2004), since N also constitutes an important structural component for fungi and is necessary for their metabolic activity (Lamour *et al.*, 2000). Data from experiments with fungal isolates indeed show positive effects of N availability on fungal activity and litter decomposition (Allison *et al.*, 2009; Osono, 2015), while experimental nitrogen additions to natural soil and litter communities show disparate findings on decomposition rates and fungal abundance (e.g. de Vries *et al.*, 2006; Meidute *et al.*, 2008; Frey *et al.*, 2014; Koranda *et al.*, 2014). Observational studies in soil are not only influenced by the complexity of microbial communities and substrate heterogeneity, but also factors shifting concurrently with N availability, for example, substrate quality, pH or other elements (Hättenschwiler *et al.*, 2011). The precise effects of N availability on fungal growth and activity will only be understood when growth traits related to N limitation are known in more detail, knowledge that can only be gained in controlled laboratory experiments.

Such controlled experiments using defined growth media have generally confirmed negative effects of N deficiency on fungal growth; however, such experiments are methodologically challenging. N amendments often exceed ecologically meaningful concentrations (Itoo and Reshi, 2014; Hoa and Wang, 2015), medium choice is arbitrary (Maynard *et al.*, 2017), co-varying factors like P or C prevent direct interpretation of N effects (Paustian and Schnürer, 1987b; Matsuura, 2002) and observed outcomes depend on the type of traits assessed (Fransson *et al.*, 2007) and are often specific to few, often only one species included in any one study (e.g. Matsuura, 2002). Especially multidimensional trait responses are not well understood, though recent trait-based approaches revealed species-specific differences in mycelial growth dynamics and enzymatic capacities (Crowther *et al.*, 2014; Lehmann *et al.*, 2019), which may also depend on substrate quality. The relatively limited representation of fungal growth responses to nutrient limitation in the plethora of emerging growth models further illustrates an apparent knowledge gap. These models are becoming increasingly sophisticated, incorporating 3D growth of fungi in heterogeneous soil environments, tip growth dynamics, branching and even nutrient translocation within mycelia, by that representing a powerful tool for predicting fungal dynamics in soil (Davidson

*et al.*, 2011). However, substrate quality is, if at all, usually only modelled for C, and even here assumptions are not well supported by data, focusing on tip growth correlations with substrate carbon supply only, due to a lack of knowledge on physiological adaptations in fungal growth (Boswell, 2008; Jeger *et al.*, 2008).

We here aim to provide such detailed knowledge on trait-based responses of saprobic fungi to nutrient limiting conditions. To achieve this, we developed a special nutrient gradient test in defined agar medium. We used it to test for responses to decreasing N (and P) supply in several saprobic fungal isolates, covering different phyla within the Eumycota. Specifically, we developed a medium based on the law of the minimum and stoichiometric theory. Taking into account the law of the minimum is highly relevant with single species growing on defined uniform medium (Danger *et al.*, 2008): all elements and conditions must be provided in nonlimiting supply to avoid masking fungal responses to deviations in nutrient supply due to the presence of other (unknown) limiting factors (Fig. 1A). Furthermore, we manipulated N supply based on molar C:N ratios mimicking a realistic range occurring in litter substrate (McGroddy *et al.*, 2004). Using such an experimental design, we evaluated the responses in biomass, extension rate, mycelial density and spore production of 16 isolates in response to C:N of 5–200. Additionally, on a subset of fungal isolates we determined detailed hyphal traits as well as activity (enzymatic activity, respiration and CUE). Using this approach, we tested the hypotheses that (i) all fungal traits reflecting growth rate and activity are negatively affected by nitrogen deficiency to a similar extent; and (ii) fungal isolates respond to N limiting conditions in a phylogenetically conserved fashion.

## Results

### *Fungal biomass, density and extension rate at different C:N supply ratios*

Fungal growth clearly differed among N supply ratios and all fungi showed responses to the N gradient in their expression of different traits (Fig. 2), as also visually apparent (Fig. S1). Not only biomass production, but also hyphal extension, density as well as other traits like colour (visual examination) differed among treatments (Fig. S1). When analysing response curves of different dependent variables, biomass showed growth peaks in the range of C:N of 100 up to 5 [on average 47.0 (27, 75) (numbers in brackets give respective variances – see Fig. 1B)]. By contrast, extension rates usually showed a maximum at high C:N values (i.e. low N supply), on average at a C:N of 163.5 (78, 200), whereas fungal density

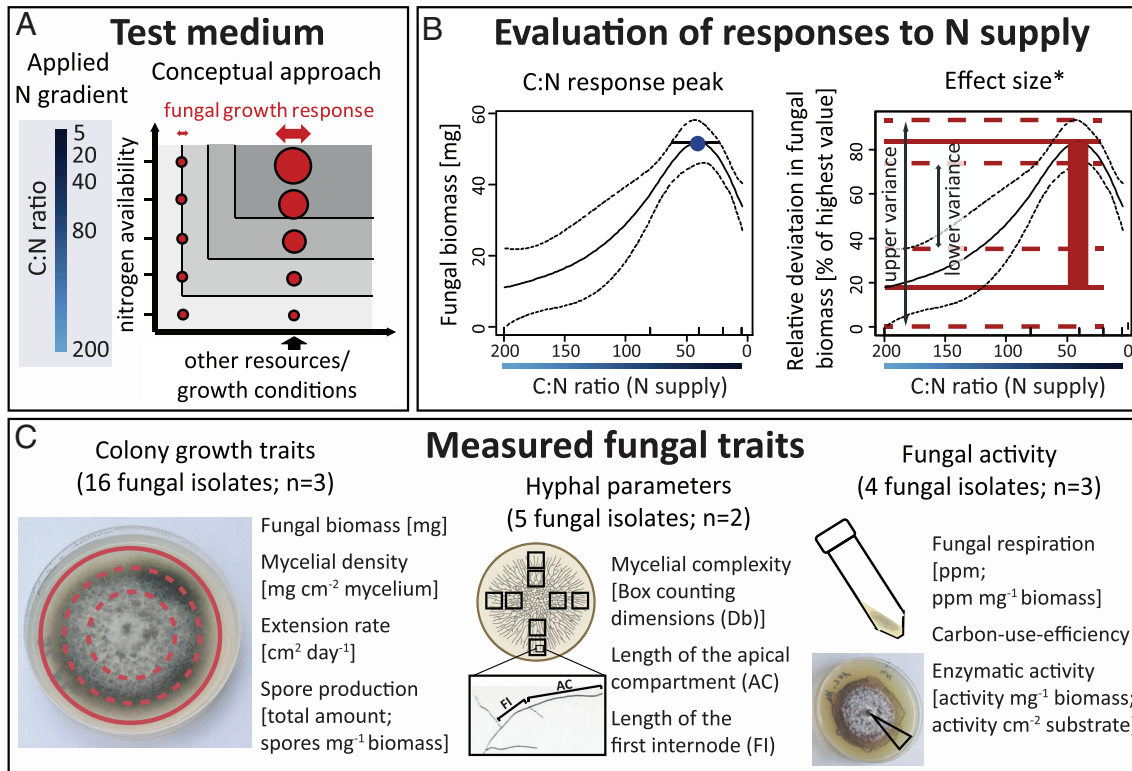


**Fig 1.** Overview of methods applied to test for trait-based fungal responses to varying N supply. A. Conceptual framework for the development of a growth medium to test for nitrogen (N) demands of different fungal isolates. The applied N gradient with tested molar C:N ratios is shown, the blue bar represents the amount of N supply (dark blue: high N content; light blue: low N content). The graph depicts the conceptual idea to design an experimental medium providing all elements and conditions in non-limiting supply, in order to allow for fungal responses to varying N supply according to the Law of the Minimum (modified from Tilman 1982). Grey areas indicate the extent of growth limitation by both, N supply as well as other resources or growth conditions (light grey: strong growth limitation; dark grey: unlimited growth). Magnitude of fungal growth response (deviations of growth in low N versus high N supply media) is illustrated by the size of red dots. B. An exemplary response curve of fungal biomass in response to varying N supply is depicted. C:N response peaks (and according variances) are derived by curve maxima based on generalized additive mixed effects models (*gamm()*) – lines indicate smoothed splines of response variables in response to differing C:N ratios, dashed lines respective 95% confidence intervals. Effect sizes were calculated based on curves depicting the relative deviation in fungal biomass (percentage of the highest value of the analysed trait for each isolate respectively). The difference among maximum relative values at high N supply and minimum relative values in low N supply represents the effect size (magnitude of fungal trait response, see Eq. 1); maximum and minimum deviations of respective 95% confidence intervals were analysed to obtain upper and lower variances. Asterisk indicates that effect sizes were only calculated for the response in fungal biomass and density. C. All measured fungal response traits are depicted, including the number of isolates and repetitions analysed. Red circles illustrate the documentation of colony extension, black squares the position of microscopic pictures taken and the black triangle circle segments sampled for enzymatic analyses. For more details, see respective methods sections. [Color figure can be viewed at [wileyonlinelibrary.com](http://wileyonlinelibrary.com)]

peaked at highest N levels [on average C:N of 5 (5, 14)] (Fig. 2). Consequently, relative changes in biomass production in most fungal isolates appeared as a trade-off between responses in extension rate and mycelial density, since biomass peaks represented intermediate values (Fig. 2). This trade-off was supported by two-way correlation analyses of relative changes in biomass with relative changes in density and extension rate: 10 out of 15 analysed isolates showed an interactive response in biomass to density and extension rate and were defined as growth response type A (Fig. 2). Only few isolates showed different strategies, namely, a positive correlation in the relative change in biomass with density, and

negative with extension rate (type B, Fig. 2) or a positive correlation with density or extension rate alone (types C and D, Fig. 2).

#### *Isolate-specific responses in effect sizes of fungal growth to increasing N supply*

Effect sizes in fungal biomass and mycelial density in response to increasing N supply ranged from 14% to 86% in biomass production, and 14% to 81% in mycelial density for different fungal isolates tested (Fig. 3). The effect sizes of biomass production and mycelial density were correlated ( $R^2 = 0.37$ ,  $p < 0.01$ ).

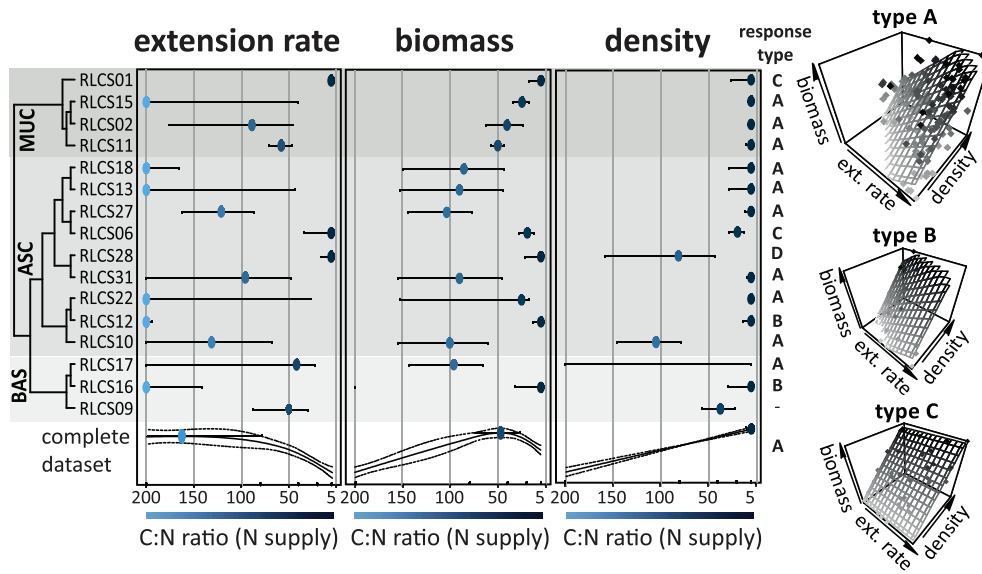


**Fig 2.** Representation of peaks in mycelial extension, biomass and density of different fungal isolates along a gradient of N supply, as well as the overall response of all fungal isolates [including the underlying model – lines indicate smoothed splines of response variables in response to differing C:N ratios, dashed lines respective 95% confidence intervals (generalized additive mixed models *gamm()*). Blue dots indicate the response peak, the corresponding lines are variances as calculated by *gamm* models (Fig. 1B), colour intensity depicts N supply rates. Continuous lines delineate fungal isolates with no responses for the respective trait. The intensity of background shading denotes phylogenetic affiliation of isolates tested. Three-dimensional scatterplots illustrate the two-way linear correlations of relative changes in biomass with relative changes in density and extension rate; shading of data points correspond to biomass values. Four response types are defined – type A comprises isolates characterized by a significant interaction term, and positive effects of both, density and extension rate on fungal biomass; type B corresponds to isolates with positive correlations of biomass with density and negative with extension rates; type C indicates that fungal biomass is only positively correlated with density and type D (graph not shown) only with extension rate. Letters indicate the response types for each fungal isolate. [Color figure can be viewed at [wileyonlinelibrary.com](http://wileyonlinelibrary.com)]

Fungal isolates showed clear differences with respect to the effect size of growth responses to varying N supply (Fig. 3), differences which were phylogenetically conserved: the phylogenetic signal expressed as Pagel's  $\lambda$  was 1.0 and 0.86 for fungal biomass and density effect sizes respectively (Fig. 3). By contrast, growth response peaks of different traits and observed response strategies to limited N conditions were highly isolate specific, but lacking a phylogenetic signal (Pagel's  $\lambda < 0.0001$ ; Fig. 2).

The correlation of different response traits (see Figs. 2 and 3) revealed that effect sizes in fungal biomass and density negatively correlated with C:N peaks of extension rates of the respective fungal isolate ( $R^2 = 0.28$ ,  $p = 0.02$  and  $R^2 = 0.76$ ,  $p < 0.001$ ), indicating that fungal strains with increased extension rates under N-limited conditions were less affected in terms of growth reduction.

#### Hyphal elongation and mycelial complexity

Detailed morphological hyphal analyses supported the responses we observed in fungal colony growth regarding extension rates versus mycelial density along different N supply ratios. Two fungal isolates characterized by decreasing extension rates at high N supply (RLCS11, RLCS27; Figs. 2 and 4A) also showed significantly decreased length of the apical compartment and the first

internode with rising N concentrations (Table S5, Fig. 4B). In parallel to the concomitant increase in mycelial density, mycelial complexity (Db) increased at high N conditions (– Table S5). By contrast, two fungal isolates characterized by a different strategy (RLCS01, RLCS28; Fig. 2), namely, increasing mycelial extension with high N supply, showed no linear decrease in the length of hyphal tips and the first internode (Table S5).

Box counting dimensions (Db) as a measure of mycelial complexity mostly reflected isolate-specific responses in mycelial density along the N gradient (Table S5, Fig. 2).

#### Spore production

Only 6 out of 16 tested fungal isolates produced spores within the given experimental period, and spore production in three isolates was restricted to a few plates or replicates (Table S6). In parallel to biomass production, the strongly sporulating isolate RLCS01 showed an increase in response with N supply in its overall amount of spores produced, as well as in spores  $\text{mg}^{-1}$  biomass, while RLCS18 and RLCS13 showed peaks at lower N supply (C:N = 29–78; Table S6). When analysing the complete data set, total spore production showed a clear linear increase with N supply as well as the amount of spores  $\text{mg}^{-1}$  fungal biomass ( $p < 0.001$ ).

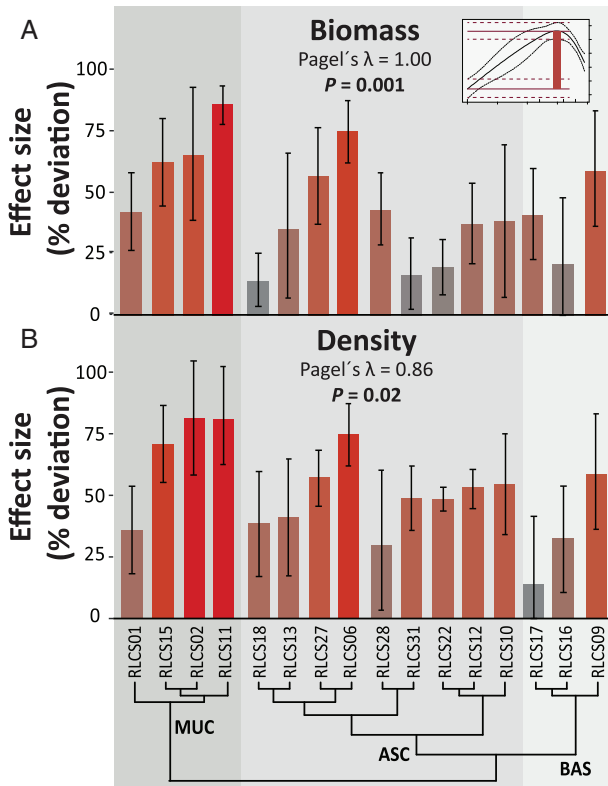


**Fig 3.** A,B. Effect sizes for fungal biomass (A) and density (B) in response to increasing N supply, calculated as given in Equation 1. Bars represent the average effect size of each fungal isolate, error bars respective lower and upper variances (see Fig. 1B). Bar colours emphasize effect sizes visually (grey: low effect size; dark red: high effect size). The insert depicts the average response in fungal biomass to N supply of all fungal isolates, as an example of effect size calculations as given by the plotted lines. The intensity of background shading denotes phylogenetic affiliation of isolates tested. [Color figure can be viewed at [wileyonlinelibrary.com](http://wileyonlinelibrary.com)]

### Enzymatic activity

With rising N supply in tested growth media, the biomass-specific fungal enzymatic activity was increased for leucine-aminopeptidase (LEU;  $p < 0.05$ ), acid-phosphatase (PHO;  $p < 0.001$ ) (Fig. 5A) and laccase or cellobiohydrolase respectively (Table S7). By contrast, glucosidase (GLU) activity did not respond (Fig. 5A). However, when analysing the activity on a basis of  $\text{cm}^{-2}$  substrate, all enzymatic activities strongly increased and peaked at a C:N ratio of 5, showing much stronger divergence along the N gradient than biomass-specific responses ( $p < 0.001$ ; Fig. 5B, Table S7).

The observed responses to the applied N gradient were isolate-specific only for LEU and GLU: RLCS01 and RLCS27 showed increasing enzymatic activities for all enzymes, regarding both, its activity  $\text{mg}^{-1}$  biomass and  $\text{cm}^{-2}$  substrate (Table S7). For RLCS17 and RLCS12, however, biomass-specific LEU activity ( $\text{mg}^{-1}$  biomass) peaked at lowest N supply ( $P < 0.01$ ), as well as GLU activity in RLCS12 ( $p < 0.01$ ), though the respective activities  $\text{cm}^{-2}$  substrate still increased due to the parallel gain in mycelial density (Fig. 2, Table S7). Thus, LEU activity as an indicator of fungal N limitation was overall not enhanced in N limited conditions, neither was the ratio of LEU/PHO or LEU/GLU activity.

### Respiratory activity and CUE

The four fungal isolates grown on 5 ml growth medium for only 5 days to measure respiratory activity showed similar growth responses as when grown on plates ( $\sim 30$  ml) for a longer period (Table S8, Fig. 2). In parallel

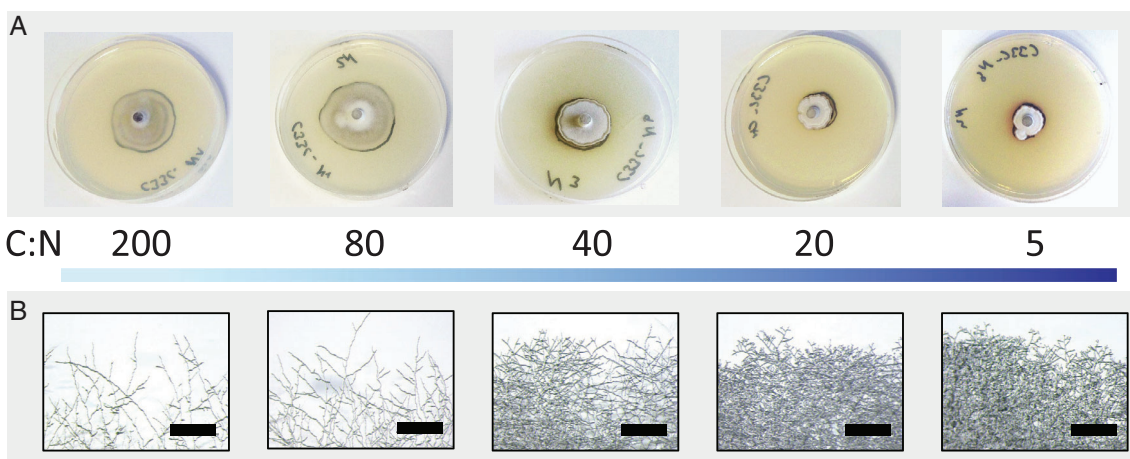


**Fig 4.** Illustration of typical fungal growth traits along the tested N gradient (see also Fig. S1). A. Pictures of mycelial growth on agar medium (RLCS27). B. Microscopic visualization of hyphal growth and mycelial structure (RLCS11; black scale bar = 200  $\mu\text{m}$ ). [Color figure can be viewed at [wileyonlinelibrary.com](http://wileyonlinelibrary.com)]

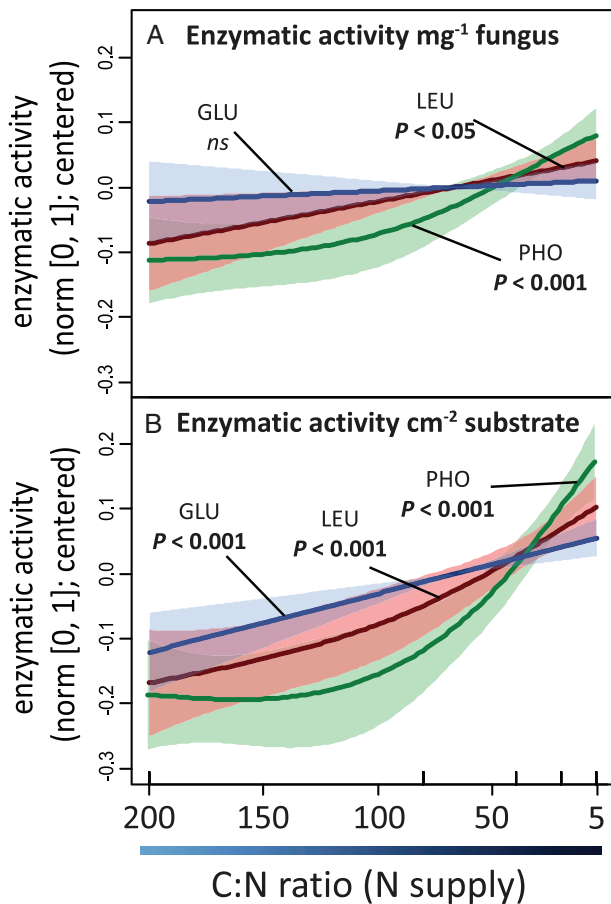


**Fig 5.** Responses in fungal enzymatic activity to increasing N supply, testing the activity of leucine-aminopeptidase (LEU; red), acid-phosphatase (PHO; green) and beta-glucosidase (GLU; blue). A,B. Fungal activity is illustrated as enzymatic activity  $\text{mg}^{-1}$  fungal biomass (A) and enzymatic activity  $\text{cm}^{-2}$  substrate colonized by fungal mycelium (B), normed in the range [0, 1] for comparisons among enzymes. Lines indicate smoothed splines of response variables in response to different C:N ratios, shaded areas respective 95% confidence intervals (generalized additive mixed models). [Color figure can be viewed at [wileyonlinelibrary.com](http://wileyonlinelibrary.com)]

with fungal biomass and density, total  $\text{CO}_2$  respired increased with N supply ( $p < 0.001$ ; Fig. 6A, Table S8). In addition to total  $\text{CO}_2$  respired, also  $\text{CO}_2 \text{ mg}^{-1}$  biomass respired increased along the N gradient, resulting in decreasing values of CUE ( $p < 0.001$ ; Fig. 6B, Table S8). Although responses were similar in RLCS01, the isolate was excluded from analyses since  $\text{CO}_2$  production exceeded detectable values, potentially resulting in  $\text{O}_2$  limitations and biased responses in activity.

#### Fungal trait responses to P and C limiting conditions

Fungal morphological responses to an applied P gradient showed trait-based patterns similar to what we observed for N (Supporting Information Appendix S2). The highest

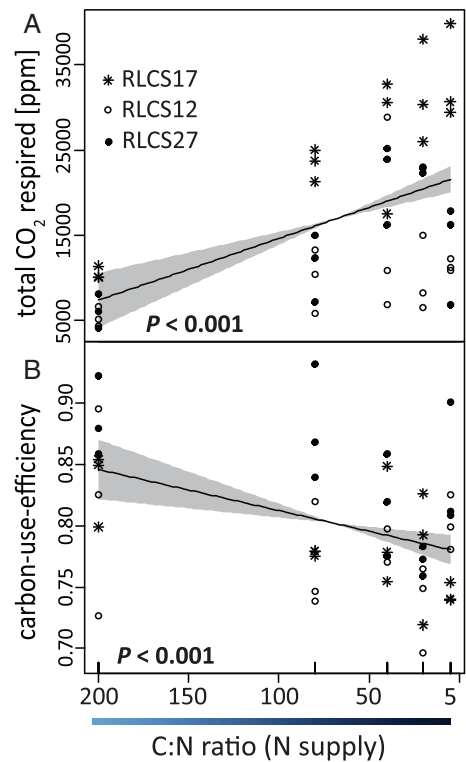


**Fig 6.** A,B. Responses in fungal respiration and carbon-use-efficiency (CUE) to increasing N supply, illustrating (A) total respiration within the experimental period of 5 days and (B) fungal carbon-use-efficiency. Lines indicate smoothed splines of response variables in response to different C:N ratios, shaded areas are 95% confidence intervals (generalized additive mixed models). Individual symbols represent data points, shapes respective fungal isolates. [Color figure can be viewed at [wileyonlinelibrary.com](http://wileyonlinelibrary.com)]

P concentration in growth media (C:P = 20) represented an optimal P supply for fungal biomass and density for all species, while extension rates were on average highest at lowest P supply (C:P = 3000, Fig. S4). Though not as pronounced as seen along the N gradient, for some species and for the complete data set the same trade-off for biomass production as described above was detected (for details, see Supporting Information Appendix S2).

Regarding the tested C gradient used for adjustments of the medium, surface area as a proxy for extension rate likewise showed overall higher values in C-limiting conditions, and clearly diverged from responses observed in fungal density and biomass (Fig. S6).

#### Discussion

All 16 fungal isolates strongly responded to a reduction in N availability, though assessed trait response curves varied among isolates and traits. Overall, fungi growing in N-limited medium had sparse, rapidly expanding mycelia with low activity. By contrast, in high N supply mycelial extension was more limited; increased branching

intensity and cross-linking led to more compact, dense mycelial growth with high enzymatic activity and respiration, collectively resulting in strongly increased enzyme activity per area of substrate colonized. Such plasticity within fungal isolates in response to nutrient supply likely contributes to efficient exploitation of heterogeneous environments in soils, with the contrast between rapid hyphal expansion and densely growing hyphae illustrating shifts from exploration to exploitation (Moore *et al.*, 2011; Veresoglou *et al.*, 2018). The same findings in morphological trait responses were also observed along a gradient of P availability as well as in preliminary experiments with varying glucose supply, indicating that this trait pattern may be universal to nutrient limiting conditions. Growth response curves, trait-based response types and effect sizes in response to N limitations varied for some isolates, but only in case of effect size a phylogenetic signal was detected.

Not supporting our first hypothesis, responses in fungal growth and activity to N availability strongly depended on the trait measured. Biomass production as a common predictor of fungal fitness reached its highest values on average at C:N of 47, though this varied among isolates. Interestingly, this value corresponds to expected N demands based on known fungal C:N ratios ( $\sim 20$ ), assuming that about half of the C is respired (Zhang and Elser, 2017; own unpublished data). By contrast, colony extension rate and hyphal tip extension, also often assessed as an indicator of fungal fitness (Score and Palfreyman, 1994; Matsuda *et al.*, 2006; Boswell, 2008), were mostly increased in nutrient limiting conditions, whereas mycelial density and branching intensity in most cases peaked at highest element supply. Correlation analyses among those traits indicate that the peak in fungal biomass at intermediate C:N values is caused by shifts in mycelial density and extension rates in opposite directions along the C:N gradient, since the relative shift in biomass in most isolates was positively correlated with both, mycelial density and extension rate. The analyses of further fungal traits, namely, spore production, enzymatic activity and respiration, revealed an overall positive linear correlation of those traits with N availability, in parallel to the increase in mycelial density as illustrated by principal component analyses (PCA) (Fig. S2). Thus, mycelial density and branching intensity as a measure of substrate exploitation intensity may be strong indicators of fungal fitness and activity in respect to nutrient supply.

The shift of explorative growth in nutrient-limited conditions towards exploitative growth in high nutrient supply has not been explicitly described before in experimental studies, but responses in extension rates to N availability have been reported to be neutral or negative (Luard, 1985; Matsuura, 2002; van Diepen *et al.*, 2017). Some authors observe 'explorative growth' in low nutrient

conditions related to branching intensity (Crawford *et al.*, 1993; Newton and Guy, 1998; Boswell, 2008), and yeasts have been reported to switch to filamentous (explorative) growth forms in limiting conditions (Amoah-Buahin *et al.*, 2005). In natural systems, beside effective exploitation of nutrient rich patches, such patterns of dense restricted mycelial colonization may also result in higher population density and contribute to co-existence among species, with positive effects on decomposition rates due to complementary growth forms and enzymatic capacities (Baldrian *et al.*, 2011; Lehmann *et al.*, 2019).

Fungal species and phylogenetic lineages not only differ in enzymatic capacities, but also nutrient demands and stoichiometric patterns (Itoo and Reshi, 2014; Zhang and Elser, 2017). Therefore, we hypothesized a phylogenetic conservation in response traits. We found clear differences among isolates, also regarding N versus P demands, as reported previously in studies testing different fungal species (Luard, 1985). Especially the deviation in only few isolates from typical trait response types, namely a different strategy to adjust explorative growth, spore production or enzymatic activity to nutrient limiting conditions may provide interesting insights for fungal community ecology, regarding differential niche breadth, dispersal or competition in heterogeneous habitats (Jiao and Lu, 2020). However, only effect size in biomass production and mycelial density showed a phylogenetic signal. Effect sizes in microbial responses are rarely reported in environmental gradients, but as an indicator of growth depression in limiting conditions may best represent actual N demands for growth of individual species (McGill *et al.*, 2006; Maynard *et al.*, 2015). The previously observed phylogenetic signal and correlation with fungal growth rates in fungal strategies of exploration versus exploitation were not confirmed by our results (Veresoglou *et al.*, 2018), but the subset of fungal isolates (16) used here may be insufficient to detect such patterns.

N is often discussed as a main structural component for fungi, also due to the occurrence of chitin. However, chitin  $[(C_8H_{13}O_5N)_n]$  only accounts for approximately 1% to 20% of fungal cell wall components (Peter, 2005). Paustian and Schnürer (1987a) estimate about 2% of N to be bound in cell walls, while 60% to 70% are found in proteins (Cochrane, 1958). Thus, we hypothesized a tight coupling of N supply and fungal activity, which our results confirmed. As reported previously under controlled conditions, fungal activity increased with N supply (Paustian and Schnürer, 1987b; Allison *et al.*, 2009). In most isolates tested, even the production of leucine-aminopeptidase, an enzyme related to N uptake was enhanced, most likely due to an overall stimulated metabolism. As a result, the ratio LEU/PHO, which is often used in enzymatic stoichiometry, did not prove to be an indicator

of fungal N limitation (Sinsabaugh *et al.*, 2008). In parallel with enzymatic activity, respiration rates increased, even when calculated per gram of fungus. Consequently, CUE was higher in low N media, indicating high C storage in biomass under abundant C supply (high C:N) (Manzoni *et al.*, 2012). Those findings of metabolic activity contradict common assumptions and observations of soil microbial activity in low N substrates (Craine *et al.*, 2007). Potentially, responses in microbial activity in complex organic substrate may deviate from results obtained in controlled inorganic medium, since access to elements is more costly and other (co-)limitations, especially by C, act on fungal activity (Schimel and Weintraub, 2003; Averill, 2014). Still, these results will help us understand enzyme allocation patterns in soil, showing strong N demands of overall enzymatic activity in fungi (Averill, 2014). Also, the apparent decoupling of enzymatic activity and biomass production observed here adds novel perspectives on mass-based fungal: bacterial ratios, which potentially underestimate fungal enzymatic contributions (Waring *et al.*, 2013).

Our experimental set-up was designed to isolate the N-limitation effect and provide a gradient of available C:N supply. In soil organic substrates, C:N ratios may not necessarily correspond to the availability of these elements (Cherif, 2012). Consequently, the applied design required element supply in easily available form. In natural soil substrate complexity will increase at multiple levels compared with growth conditions applied here, regarding patchy distributions of heterogeneous organically bound substrate, differential element limitations, fungal communities operating collectively and interactions with other organism groups (Falconer *et al.*, 2005; Crowther *et al.*, 2018). In future studies, the experimental system introduced here can be used to evaluate impacts of this complexity on experimental outcomes.

In conclusion, our results highlight strong fungal responses in growth and activity to nitrogen-limiting conditions, revealing clear trait-based patterns. Findings point towards a mechanism explaining optimal fungal substrate foraging in heterogeneous environments, since directed growth as an explanation has not been reported for fungi so far (Tlalka *et al.*, 2008). However, nutrient 'sensing' by certain membrane receptors does occur (Bahn *et al.*, 2007; Lin *et al.*, 2015), and the trait responses found here support the existence of internal fungal regulations to switch from explorative growth in low nutrient conditions to exploitative growth in nutrient rich patches. Diverging strategies in certain isolates may relate to lower N demands, as indicated by negative correlations of effect sizes with extension rate optima, or an adaptation to sporulation versus mycelial outgrowth as explorative strategy (Fricker *et al.*, 2008). Incorporating these trait-based responses in fungal growth models will

improve our ecological understanding of fungal growth and activity in complex soil substrate, while the knowledge gained on complex fungal trait indicators for limiting conditions will improve the interpretation of field studies.

## Experimental procedures

### Fungal material

In total, 16 fungal isolates were used for analyses, previously isolated from soil samples originating from a grassland site in northern Germany ('Oderhänge Mallnow' close to the town of Lebus, Germany; 52°13'N, 14°13'E) (Andrade-Linares *et al.*, 2016), hereinafter called the Rillig Lab Core Set (RLCS). Included fungal strains comprised four Mucoromycota, three Basidiomycota and nine Ascomycota; details on DSMZ accession numbers (German Collection of Microorganisms and Cell Cultures GmbH) and phylogenetic affiliations are provided in Table S1 (for details of the phylogeny, see Lehmann *et al.*, 2019). Table S2 gives a detailed overview which isolates were used for each trait measurement (see Fig. 1). Before the experiment, each isolate was divided into three repetitions and cultured separately on potato dextrose agar with antibiotics to eliminate potential contaminants. Subsequently, repetitions were transferred to water agar (1.5%), in order to reduce nutrient storage in fungal tissues. Unless indicated otherwise, all three repetitions were analysed separately for each fungal isolate and treatment.

### Experimental design

In accordance with the law of the minimum we designed an experimental medium providing all elements and conditions in non-limiting supply (Fig. 1A), based on common growth media and several pre-tests (Hoefnagels, 2005, see Supporting Information Appendix S1 for details). The upper limit of fungal growth was standardized by C availability based on a glucose gradient test (see for further details and rationales Supporting Information Appendix S1, Table S3). The derived medium contained 5 g L<sup>-1</sup> glucose, 0.2 g L<sup>-1</sup> NaH<sub>2</sub>PO<sub>4</sub> (C:P = 100), 0.5 g L<sup>-1</sup> MgSO<sub>4</sub>, 0.5 g KCl, 0.1 g NaFeEDTA, 5 mg L<sup>-1</sup> ZnSO<sub>4</sub>, 0.05 mg L<sup>-1</sup> Na<sub>2</sub>Mo<sub>4</sub>, 0.05 mg L<sup>-1</sup> MnSO<sub>4</sub>, 0.05 mg L<sup>-1</sup> H<sub>3</sub>BO<sub>4</sub>, 0.01 mg L<sup>-1</sup> CuSO<sub>4</sub>, 1 mg L<sup>-1</sup> thiamine HCl, 0.05 mg L<sup>-1</sup> biotin, and 20 g L<sup>-1</sup> agar.

N supply was manipulated based on molar C:N ratios, adding NH<sub>4</sub>NO<sub>3</sub> in a defined quantity as universal fungal N source (Jennings, 1995). Five levels of N supply were tested (C:N = 5, 20, 40, 80 and 200; Fig. 1A). In order to evaluate whether observed fungal responses to N limitation generally apply to nutrient limitations, P supply was also manipulated in a separate experiment [C:P = 20,

100, 5000, 1000, 3000 (C:N = 20)]; results are presented in Supporting Information Appendix S2). Levels of high nutrient supply were based on expected fungal demands derived from published C:N:P contents (Mouginot *et al.*, 2014; Zhang and Elser, 2017), whereas values for low nutrient supply were based on lower limits reported in litter and soil (McGroddy *et al.*, 2004; Cleveland and Liptzin, 2007).

For media preparation, glucose and phosphate were autoclaved separately, since glucose may caramelize in the presence of salts, and phosphate forms insoluble precipitates or provokes toxic conditions (Moore *et al.*, 2011; Tanaka *et al.*, 2014).  $\text{NH}_4\text{NO}_3$  or  $\text{NaH}_2\text{PO}_4$  additions did not change the pH of the base medium ( $\sim 4.5$ ). In case of manipulations of P supply,  $16 \text{ g L}^{-1}$  special purified agar was used [A7921, Sigma-Aldrich, Darmstadt, Germany;  $0.04 \text{ mg P g}^{-1}$  agar (ICP-OES analysis)].

Fungi were grown in petri dishes in the dark for 12 days at  $20^\circ\text{C}$  ( $\varnothing 9 \text{ mm}$ ), only the fast-growing isolate RLCS01 was kept for 7 days to avoid spatial limitation (Fig. 1A), while RLCS28 and RLCS31 were grown for 27 days to obtain sufficient growth.

#### *Fungal traits assessed as response variables*

**Biomass** – At the end of the experiment, agar media were melted and mycelium collected on a  $20 \mu\text{m}$  mesh. Fungi were freeze-dried to determine dry fungal biomass.

**Extension rate** – At the end of experiment, as well as at least once during fungal growth, the outer limit of mycelial extension was marked (Fig. 1C). Total area at different dates was determined with the image-analysis program ImageJ (Schneider *et al.*, 2012) by encircling the whole colony. For each fungal isolate and treatment, growth curves were created to calculate extension rates (colony extension in  $\text{cm}^2 \text{ day}^{-1}$ ) within linear colony extension.

**Density** – Fungal density [ $\text{mg cm}^{-2}$  mycelium] was calculated as the ratio of fungal biomass and complete area covered by mycelium at the end of the experiment.

**Spore production** – At the end of experiment, spores were washed off from the mycelium with 10 ml dest.  $\text{H}_2\text{O}$ . Next, 2 ml of the suspension was centrifuged (12,500 rpm for 5 min) to concentrate spores in  $200 \mu\text{l}$  solution. Then  $12 \mu\text{l}$  was used for spore counting using a Neubauer chamber at  $400\times$  magnification. Total spore abundance (per plate) and abundance per gram fungal biomass were calculated.

**Hyphal parameters** – Several fungal isolates were grown additionally on thin layers of media [ $2 \text{ ml plate}^{-1}$  ( $\varnothing 6 \text{ mm}$ )], in order to analyse hyphal tip growth and mycelial development in detail. Five fungal isolates showing different trait response types to the applied N gradient were selected (Fig. 2; RLCS11, RLCS01, RLCS28,

RLCS27, RLCS10), for which image analyses were possible under our conditions. Two repetitions of each isolate were analysed, and microscopic pictures taken at four random locations at the outer edge of the colony for each plate, as well as in the inner part (at half of the mycelial diameter; Fig. 1C). Microscope settings were kept fixed for each isolate independent of N supply. Using ImageJ (Schneider *et al.*, 2012), five single hyphae at the outer mycelial edge were analysed for each picture, measuring the length from hyphal tip up to the first branch (hereafter referred to as apical compartment) as well as the length of the first internode (Fig. 1C). Mycelial complexity (i.e. the degree of detail) of the inner and outer mycelium was determined by box counting dimensions (Db; for details see Supporting Information Appendix S1).

**Enzymatic activity** – Fungal enzymatic activity was determined following a microplate photometric method according to a modified protocol by Zheng *et al.* (in press). Due to time requirements of this method, only four isolates (RLCS01, RLCS17, RLCS12 and RLCS27) were tested, selected based on their phylogenetic coverage. Four enzymes were tested for each isolate – laccase, beta-glucosidase, leucine-aminopeptidase and acid-phosphatase. In case of RLCS01, laccase was replaced by cellobiohydrolase, since no laccase activity was recorded. For each enzyme tested, a piece of mycelium was cut as a circle segment of the colony (Fig. 1C) in order to obtain enzymatic activity representative of the whole fungal colony. Detailed information on conditions and substrates are given in Table S4 and Supporting Information Appendix S1.

**Respiration/CUE** – The same four fungal isolates tested for enzymatic activity were grown in 50 ml falcon tubes on 5 ml of media differing in C:N ratios, for analyses of fungal respiration (Fig. 1C). We chose these conditions, that is, a small volume of medium, the short growth period of 5 days and air sampling every 2 days, to avoid oxygen limitation as well as  $\text{CO}_2$  concentrations exceeding detection limits.  $\text{CO}_2$  production was measured with the Licor Li-6400XT system. Carbon-use-efficiency was calculated based on the formula given by Maynard *et al.* (2017) – dividing the net amount of C in biomass by the total amount of C that was either respired or incorporated into biomass [fungal C content was determined in fungi grown for 12 days with an Elemental Analyser (EuroEA, HekaTech, Germany)].

#### *Statistical analyses*

First, we analysed the responses of each observed fungal trait to the applied N gradient independently. Since the correlations of most measured traits with nutrient availability were non-linear and followed different distributions depending on isolates and traits assessed, effects

of nutrient supply were analysed by generalized additive mixed models using the function *gamm()* (package *mgcv*; Verbeke, 2007). Here, the function is specified non-parametrically as 'smooth function'. For most analyses, *gaussian* distribution was assumed, while for skewed data *gamma* distribution with log link was used, and for data with many zeros (e.g. spore counts) *quasipoisson* or *poisson*. In case of a significant correlation of tested traits with nutrient availability, the peak of the *gamm* output was determined to investigate the growth responses of different fungal traits; variance was given according to the width of 95% confidence intervals (see Fig. 1B). Trait responses were analysed for individual fungal isolates taking repetition as random factor, as well as for all fungal isolates collectively using isolate identity and repetition as random factors. The alternative inclusion of phylogenetic structure of isolates in a random slope model as described below did not improve model fit (evaluated by the Akaike information criterion).

In order to assess the extent of fungal responses to varying N supply, effect sizes were calculated for fungal biomass and density. Since the applied nutrient gradient does not allow for standard effect size calculations based on treatment and control values, and isolates varied in their shape of growth response curves, we used the relative deviation of fungal growth at minimal growth in low nutrient supply and its highest value reached at the respective peak of growth response (Eq. 1, Fig. 1B). Generalized additive mixed models based on relative trait values (each value expressed as the percentage of the highest value of the analysed trait for each isolate respectively) were used to calculate respective effect sizes. The shortest and widest distance of 95% confidence intervals were used to estimate lower and upper variances respectively (see Fig. 1B).

$$\text{Effect size (\%)} = \frac{\text{highest relative trait value at C:N peak} - \text{concentration (\%)} - \text{minimum relative}}{\times \text{trait value at low N supply (\%)}} \quad (1)$$

The phylogenetic signal (Pagel's  $\lambda$ ) in effect sizes and trait response peaks in biomass and density of tested fungal isolates was analysed using function *phyloSignal()* (package *phyloSignal*; Keck *et al.*, 2016). Correlations among effect sizes in biomass and density, as well as with trait response peaks were calculated by phylogenetic generalized linear models (*pgls()* in package *caper*; Orme *et al.*, 2018).

The general relations among observed fungal traits were depicted by PCA using function *prcomp()*, based on relative trait values (see above). Separate PCAs were done for traits assessed only in a subset of fungal isolates (Fig. S2). PerMANOVA analyses approved the

significant responses of all depicted trait combinations to N manipulation [function *adonis()* (package *vegan*; Oksanen *et al.*, 2013)]. Additionally, the correlation among specific growth traits, namely biomass with density and extension rate were explored by two-way linear mixed-effects models using the function *lme()* [package *nlme* (Pinheiro *et al.*, 2020)]. Phylogenetic covariance and isolate identity were used as random slope and intercept respectively. For phylogenetic covariance structure, we used the first axis (54% explained variance) of a PCA based on the variance-covariance matrix of the phylogenetic tree (*vcv.phylo()* in package *ape*; Paradis and Schliep, 2018). Here, again relative deviations within isolate for each trait were calculated to normalize data for comparisons. In case of non-normality, data were log-transformed. We generated 3D scatterplots using the package *plot3D* (Soetaert, 2017). Based on these results we defined four possible 'growth response types' (see Fig. 2), characterizing the relations among growth traits in response to varying N supply within individual fungal isolates.

All analyses were done in R version 3.6.1 (R Core Team, 2019).

## Acknowledgement

We thank Masahiro Ryo for statistical advice, and Carlos Aguilar-Trigueros for general methodological support. M. C. R. acknowledges financial support from an ERC Advanced Grant (694368).

## References

- Allison, S.D., LeBauer, D.S., Ofrecio, M.R., Reyes, R., Ta, A. M., and Tran, T.M. (2009) Low levels of nitrogen addition stimulate decomposition by boreal forest fungi. *Soil Biol Biochem* **41**: 293–302.
- Amoah-Buahin, E., Bone, N., and Armstrong, J. (2005) Hyphal growth in the fission yeast *Schizosaccharomyces pombe*. *Eukaryot Cell* **4**: 1287–1297.
- Andrade-Linares, D.R., Veresoglou, S.D., and Rillig, M.C. (2016) Temperature priming and memory in soil filamentous fungi. *Fungal Ecology* **21**: 10–15.
- Augusto, L., Achat, D.L., Jonard, M., Vidal, D., and Ringeval, B. (2017) Soil parent material – a major driver of plant nutrient limitations in terrestrial ecosystems. *Glob Chang Biol* **23**: 3808–3824.
- Averill, C. (2014) Divergence in plant and microbial allocation strategies explains continental patterns in microbial allocation and biogeochemical fluxes. *Ecol Lett* **17**: 1202–1210.
- Averill, C., and Waring, B. (2018) Nitrogen limitation of decomposition and decay: How can it occur? **24**: 1417–1427.
- Bahn, Y.S., Xue, C.Y., Idnurm, A., Rutherford, J.C., Heitman, J., and Cardenas, M.E. (2007) Sensing the environment: lessons from fungi. *Nat Rev Microbiol* **5**: 57–69.

- Baldrian, P., Voriskova, J., Dobiasova, P., Merhautova, V., Lisa, L., and Valaskova, V. (2011) Production of extracellular enzymes and degradation of biopolymers by saprotrophic microfungi from the upper layers of forest soil. *Plant and Soil* **338**: 111–125.
- Boddy, L. (1999) Saprotrophic cord-forming fungi: meeting the challenge of heterogeneous environments. *Mycologia* **91**: 13–32.
- Boswell, G.P. (2008) Modelling mycelial networks in structured environments. *Mycol Res* **112**: 1015–1025.
- Cherif, M. (2012). Biological Stoichiometry: The Elements at the Heart of Biological Interactions. A. Innocenti *Stoichiometry and Research - The Importance of Quantity in Biomedicine*, (357–376). Rijeka, Croatia: INTECH Open Access Publisher.
- Cleveland, C.C., and Liptzin, D. (2007) C: N: P stoichiometry in soil: is there a 'Redfield ratio' for the microbial biomass? *Biogeochemistry* **85**: 235–252.
- Cochrane, V. (1958) *Physiology of Fungi*. New York, NY, USA: Wiley.
- Cooke, R., and Whipps, J. (1993) *Ecophysiology of Fungi*. Oxford, Boston: Blackwell Scientific Publications.
- Coskun, D., Britto, D.T., and Kronzucker, H.J. (2016) Nutrient constraints on terrestrial carbon fixation: the role of nitrogen. *J Plant Physiol* **203**: 95–109.
- Craine, J.M., Morrow, C., and Fierer, N. (2007) Microbial nitrogen limitation increases decomposition. *Ecology* **88**: 2105–2113.
- Crawford, J.W., Ritz, K., and Young, I.M. (1993) Quantification of fungal morphology, gaseous transport and microbial dynamics in soil – an integrated framework utilizing fractal geometry. *Geoderma* **56**: 157–172.
- Crowther, T.W., Boddy, L., and Maynard, D.S. (2018) The use of artificial media in fungal ecology. *Fungal Ecology* **32**: 87–91.
- Crowther, T.W., Maynard, D.S., Crowther, T.R., Peccia, J., Smith, J.R., and Bradford, M.A. (2014) Untangling the fungal niche: the trait-based approach. *Front Microbiol* **5**: UNSP 579.
- Danger, M., Daufresne, T., Lucas, F., Pissard, S., and Lacroix, G. (2008) Does Liebig's law of the minimum scale up from species to communities? *Oikos* **117**: 1741–1751.
- Davidson, F.A., Boswell, G.P., Fischer, M.W.F., Heaton, L., Hofstadler, D., and Roper, M. (2011) Mathematical modelling of fungal growth and function. *IMA Fungus* **2**: 33–37.
- de Vries, F.T., Hoffland, E., van Eekeren, N., Brussaard, L., and Bloem, J. (2006) Fungal/bacterial ratios in grasslands with contrasting nitrogen management. *Soil Biol Biochem* **38**: 2092–2103.
- Elser, J.J., Dobberfuhl, D.R., MacKay, N.A., and Schampel, J.H. (1996) Organism size, life history, and N:P stoichiometry. *Bioscience* **46**: 674–684.
- Falconer, R.E., Bown, J.L., White, N.A., and Crawford, J.W. (2005) Biomass recycling and the origin of phenotype in fungal mycelia. *Proceedings of the Royal Society B-Biological Sciences* **272**: 1727–1734.
- Falconer, R.E., Bown, J.L., White, N.A., and Crawford, J.W. (2007) Biomass recycling: a key to efficient foraging by fungal colonies. *Oikos* **116**: 1558–1568.
- Fransson, P.M.A., Anderson, I.C., and Alexander, I.J. (2007) Ectomycorrhizal fungi in culture respond differently to increased carbon availability. *FEMS Microbiol Ecol* **61**: 246–257.
- Frey, S.D., Ollinger, S., Nadelhoffer, K., Bowden, R., Brzostek, E., Burton, A., et al. (2014) Chronic nitrogen additions suppress decomposition and sequester soil carbon in temperate forests. *Biogeochemistry* **121**: 305–316.
- Fricker, M.D., Bebbler, D., and Boddy, L. (2008) Chapter 1 mycelial networks: structure and dynamics. In *British Mycological Society Symposia Series*, Boddy, L., Frankland, J.C., and van West, P. (eds). Cambridge, MA, USA: Academic Press, pp. 3–18.
- Fricker, M.D., Heaton, L.L.M., Jones, N.S., and Boddy, L. (2017) The mycelium as a network. *Microbiology Spectrum* **5**: FUNK-0033-2017.
- Hartman, W.H., and Richardson, C.J. (2013) Differential nutrient limitation of soil microbial biomass and metabolic quotients (qCO<sub>2</sub>): is there a biological stoichiometry of soil microbes? *PLoS One* **8**: e57127.
- Hättenschwiler, S., Coq, S., Barantal, S., and Handa, I.T. (2011) Leaf traits and decomposition in tropical rainforests: revisiting some commonly held views and towards a new hypothesis. *New Phytol* **189**: 950–965.
- Hoa, H.T., and Wang, C.L. (2015) The effects of temperature and nutritional conditions on mycelium growth of two oyster mushrooms (*Pleurotus ostreatus* and *Pleurotus cystidiosus*). *Mycobiology* **43**: 14–23.
- Hoefnagels, M.H. (2005) Biodiversity of fungi: inventory and monitoring methods. *Bioscience* **55**: 282–283.
- Hu, S., Chapin, F.S., Firestone, M.K., Field, C.B., and Chiariello, N.R. (2001) Nitrogen limitation of microbial decomposition in a grassland under elevated CO<sub>2</sub>. *Nature* **409**: 188–191.
- Ito, Z.A., and Reshi, Z.A. (2014) Effect of different nitrogen and carbon sources and concentrations on the mycelial growth of ectomycorrhizal fungi under in-vitro conditions. *Scandinavian Journal of Forest Research* **29**: 619–628.
- Jeger, M.J., Lamour, A., Gilligan, C.A., and Otten, W. (2008) A fungal growth model fitted to carbon-limited dynamics of *Rhizoctonia solani*. *New Phytol* **178**: 625–633.
- Jennings, D.H. (1995) *The Physiology of Fungal Nutrition*. Cambridge, UK: Cambridge University Press.
- Jiao, S., and Lu, Y. (2020) Abundant fungi adapt to broader environmental gradients than rare fungi in agricultural fields. *Global Change Biol.* <https://doi.org/10.1111/gcb.15130>.
- Keck, F., Rimet, F., Bouchez, A., and Franc, A. (2016) Phylosignal: an R package to measure, test, and explore the phylogenetic signal. *Ecol Evol* **6**: 2774–2780.
- Koranda, M., Kaiser, C., Fuchslueger, L., Kitzler, B., Sessitsch, A., Zechmeister-Boltenstern, S., and Richter, A. (2014) Fungal and bacterial utilization of organic substrates depends on substrate complexity and N availability. *FEMS Microbiol Ecol* **87**: 142–152.
- Lamour, A., Van den Bosch, F., Termorshuizen, A.J., and Jeger, M.J. (2000) Modelling the growth of soil-borne fungi in response to carbon and nitrogen. *IMA J Math Appl Med Biol* **17**: 329–346.
- Lehmann, A., Zheng, W., Soutschek, K., Roy, J., Yurkov, A. M., and Rillig, M.C. (2019) Tradeoffs in hyphal traits determine mycelium architecture in saprobic fungi. *Sci Rep* **9**: 14152.

- Lin, X.R., Alspaugh, J.A., Liu, H.P., and Harris, S. (2015) Fungal morphogenesis. *Cold Spring Harb Perspect Med* **5**: a019679.
- Luard, E.J. (1985) Interaction of substrate C–N ratio and osmotic potential on growth and osmoregulation of 4 filamentous fungi. *New Phytol* **101**: 117–132.
- Manzoni, S., Taylor, P., Richter, A., Porporato, A., and Agren, G.I. (2012) Environmental and stoichiometric controls on microbial carbon-use efficiency in soils. *New Phytol* **196**: 79–91.
- Manzoni, S., Trofymow, J.A., Jackson, R.B., and Porporato, A. (2010) Stoichiometric controls on carbon, nitrogen, and phosphorus dynamics in decomposing litter. *Ecological Monographs* **80**: 89–106.
- Matsuda, Y., Sugiyama, F., Nakanishi, K., and Ito, S.-i. (2006) Effects of sodium chloride on growth of ectomycorrhizal fungal isolates in culture. *Mycoscience* **47**: 212–217.
- Matsuura, S. (2002) Colony patterning and collective hyphal growth of filamentous fungi. *Physica a – statistical mechanics and its applications* **315**: 125–136.
- Maynard, D.S., Crowther, T.W., and Bradford, M.A. (2017) Fungal interactions reduce carbon use efficiency. *Ecol Lett* **20**: 1034–1042.
- Maynard, D.S., Leonard, K.E., Drake, J.M., Hall, D.W., Crowther, T.W., and Bradford, M.A. (2015) Modelling the multidimensional niche by linking functional traits to competitive performance. *Proc R Soc B Biol Sci* **282**: 9.
- McGill, B.J., Enquist, B.J., Weiher, E., and Westoby, M. (2006) Rebuilding community ecology from functional traits. *Trends Ecol Evol* **21**: 178–185.
- McGroddy, M.E., Daufresne, T., and Hedin, L.O. (2004) Scaling of C: N: P stoichiometry in forests worldwide: implications of terrestrial Redfield-type ratios. *Ecology* **85**: 2390–2401.
- Meidute, S., Demoling, F., and Baath, E. (2008) Antagonistic and synergistic effects of fungal and bacterial growth in soil after adding different carbon and nitrogen sources. *Soil Biol Biochem* **40**: 2334–2343.
- Moore, D., Robson, G., and Trinci, A. (2011) *21st Century Guidebook to Fungi*. Cambridge, UK: Cambridge University Press.
- Mouginot, C., Kawamura, R., Matulich, K.L., Berlemont, R., Allison, S.D., Amend, A.S., and Martiny, A.C. (2014) Elemental stoichiometry of fungi and bacteria strains from grassland leaf litter. *Soil Biol Biochem* **76**: 278–285.
- Newton, A.C., and Guy, D.C. (1998) Exploration and exploitation strategies of powdery mildew on barley cultivars with different levels of nutrients. *Eur J Plant Pathol* **104**: 829–833.
- Oksanen, J., Blanchet, F.G., Kindt, R., Legendre, P., Minchin, P.R., O'Hara, R.B. et al. (2013) *R: A Language and Environment for Statistical Computing*, Vienna, Austria: R Foundation for Statistical Computing.
- Orme, D., Freckleton, R., Thomas, G., Petzoldt, T., Fritz, S., Isaac, N., and Pearse, W. (2018) Caper: Comparative analyses of phylogenetics and evolution in R. In *R Package Version 1.0.1*, Vienna, Austria: R Foundation for Statistical Computing. <https://www.R-project.org/>.
- Osono, T. (2015) Effects of litter type, origin of isolate, and temperature on decomposition of leaf litter by macrofungi. *J Forest Res* **20**: 77–84.
- Paradis, E., and Schliep, K. (2018) Ape 5.0: an environment for modern phylogenetics and evolutionary analyses in R. *Bioinformatics* **35**: 526–528.
- Paustian, K., and Schnürer, J. (1987a) Fungal growth response to carbon and nitrogen limitation – a theoretical model. *Soil Biol Biochem* **19**: 613–620.
- Paustian, K., and Schnürer, J. (1987b) Fungal growth response to carbon and nitrogen limitation – application of a model to laboratory and field data. *Soil Biol Biochem* **19**: 621–629.
- Peter, M. (2005) Chitin and chitosan in fungi. In *Biopolymers Online*, Steinbüchel, A. (ed). Weinheim, Germany: Wiley-VCH Verlag GmbH & Co. KGaA.
- Pinheiro, J., Bates, D., DebRoy, S., Sarkar, D., and Core Team, R. (2020) nlme: Linear and nonlinear mixed effects models. In *R package version 3.1-147*, Vienna, Austria: R Foundation for Statistical Computing.
- R Core Team. (2019) *R: A Language and Environment for Statistical Computing*. Vienna, Austria: R Foundation for Statistical Computing. <https://www.R-project.org>.
- Riggs, C.E., and Hobbie, S.E. (2016) Mechanisms driving the soil organic matter decomposition response to nitrogen enrichment in grassland soils. *Soil Biol Biochem* **99**: 54–65.
- Ritz, K. (1995) Growth responses of some soil fungi to spatially heterogeneous nutrients. *FEMS Microbiol Ecol* **16**: 269–279.
- Rousk, J., and Bengtson, P. (2014) Microbial regulation of global biogeochemical cycles. *Front Microbiol* **5**: 103.
- Schimel, J.P., and Weintraub, M.N. (2003) The implications of exoenzyme activity on microbial carbon and nitrogen limitation in soil: a theoretical model. *Soil Biol Biochem* **35**: 549–563.
- Schneider, C.A., Rasband, W.S., and Eliceiri, K.W. (2012) NIH image to ImageJ: 25 years of image analysis. *Nat Methods* **9**: 671–675.
- Score, A.J., and Palfreyman, J.W. (1994) Biological control of the dry rot fungus *Serpula lacrymans* by *Trichoderma* species – the effects of complex and synthetic media on interaction and hyphal extension rates. *Int Biodeter Biodegr* **33**: 115–128.
- Sinsabaugh, R.L., Lauber, C.L., Weintraub, M.N., Ahmed, B., Allison, S.D., Crenshaw, C., et al. (2008) Stoichiometry of soil enzyme activity at global scale. *Ecol Lett* **11**: 1252–1264.
- Soetaert, K. (2017) Plot3d: Plotting Multi-Dimensional Data. In *R Package Version 1.1.1*. Vienna, Austria: R Foundation for Statistical Computing.
- Spohn, M., and Chodak, M. (2015) Microbial respiration per unit biomass increases with carbon-to-nutrient ratios in forest soils. *Soil Biol Biochem* **81**: 128–133.
- Tanaka, T., Kawasaki, K., Daimon, S., Kitagawa, W., Yamamoto, K., Tamaki, H., et al. (2014) A hidden pitfall in the preparation of agar media undermines microorganism cultivability. *Appl Environ Microbiol* **80**: 7659–7666.
- Tilman, D. (1982) Resource competition and community structure. *Monogr Popul Biol* **17**: 1–296.
- Tlalka, M., Bebbler, D.P., Darrach, P.R., Watkinson, S.C., and Fricker, M.D. (2008) Quantifying dynamic resource allocation illuminates foraging strategy in *Phanerochaete velutina*. *Fungal Genet Biol* **45**: 1111–1121.

- Treseder, K.K. (2008) Nitrogen additions and microbial biomass: a meta-analysis of ecosystem studies. *Ecol Lett* **11**: 1111–1120.
- van Diepen, L.T.A., Frey, S.D., Landis, E.A., Morrison, E.W., and Pringle, A. (2017) Fungi exposed to chronic nitrogen enrichment are less able to decay leaf litter. *Ecology* **98**: 5–11.
- Verbeke, T. (2007) Generalized additive models: an introduction with R. *J R Stat Soc Ser A Stat Soc* **170**: 262–262.
- Veresoglou, S.D., Wang, D., Andrade-Linares, D.R., Hempel, S., and Rillig, M.C. (2018) Fungal decision to exploit or explore depends on growth rate. *Microb Ecol* **75**: 289–292.
- Vitousek, P.M., and Howarth, R.W. (1991) Nitrogen limitation on land and in the sea: how can it occur? *Biogeochemistry* **13**: 87–115.
- Waring, B.G., Averill, C., and Hawkes, C.V. (2013) Differences in fungal and bacterial physiology alter soil carbon and nitrogen cycling: insights from meta-analysis and theoretical models. *Ecol Lett* **16**: 887–894.
- Watkinson, S.C., Davison, E.M., and Bramah, J. (1981) The effect of nitrogen availability on growth and cellulolysis by *Serpula lacrimans*. *New Phytol* **89**: 295–305.
- Zhang, J., and Elser, J.J. (2017) Carbon:nitrogen:phosphorus stoichiometry in fungi: a meta-analysis. *Front Microbiol* **8**: 1281.
- Zheng, W., Lehmann, A., Ryo, M., Valyi, K., and Rillig, M.C. (in press) Growth rate trades off with enzymatic investment in soil filamentous fungi. *bioRxiv*: 360511. <https://doi.org/10.1101/360511>.

### Supporting Information

Additional Supporting Information may be found in the online version of this article at the publisher's web-site:

**Appendix S1.** Supporting Information 1.

**Appendix S2.** Supporting Information 2.

**Appendix S3.** Additional Data.